Estimating plastic export from estuaries into the sea using an estuarine-mass-balance model

D.M.P. van Waterschoot, S.A.J. Tas, N. Gratiot, P. Vriend, Isabel Jalón-Rojas, T.H.M. van Emmerik

Marine Pollution Bulletin 230 (2026) 119793

Contents lists available at ScienceDirect

Marine Pollution Bulletin

journal homepage: www.elsevier.com/locate/marpolbul

Estimating plastic export from estuaries into the sea using an estuarine-mass-balance model

D.M.P. van Waterschoot [a], S.A.J. Tas [a], N. Gratiot [b], P. Vriend [c,d], I. Jalón-Rojas [e], T.H.M. van Emmerik [a,*]

[a] Hydrology and Environmental Hydraulics Group, Wageningen University, Wageningen, The Netherlands
[b] Univ. Grenoble Alpes, IRD, CNRS, INRAE, Grenoble INP*, IGE, *Institute of Engineering and Management Univ. Grenoble Alpes, Grenoble, France
[c] Rijkswaterstaat, Ministry of Infrastructure and Water Management, the Hague, The Netherlands
[d] Institute of Environmental Sciences, Leiden, The Netherlands
[e] Univ. Bordeaux, CNRS, Bordeaux INP, EPOC, UMR 5805, Pessac, France

ARTICLE INFO

Dataset link: 4TU.ResearchData, https://data.4tu.nl/datasets/08735cb7-8859-4ddb-8a09-90df4d4ba1c1

Keywords:
Plastic
Estuary
Sea
Mass balance
Model
Plastic transport
Plastic deposition
Plastic remobilization
Rhine–Meuse
Saigon

ABSTRACT

Estuaries act as an interface between rivers and the sea, and therefore play a key role in transporting plastic to the sea. However, plastic transport in estuaries is complex and estuary-to-sea export is still very uncertain. This study presents a macroplastic mass-balance model that can be applied to specific estuaries, and produces export estimates similar to previous studies. The daily plastic export from estuary to sea during the wet season was estimated to be 290 kg for the Rhine–Meuse Estuary (RME), and 19,431 kg for the Saigon Estuary, where the discharge into the sea is 3.5 times larger for the RME, compared to the Saigon Estuary. Due to limited river discharge measurements for the Saigon Estuary, a yearly simulation could only be performed for the RME, corresponding to an export of 13,300 kg. These estimates fall within the uncertainty range of previous studies. Deposition and remobilization from riverbanks resulted in the largest model fluxes, with magnitudes of 20 t/d for the RME and 430 t/d for the Saigon Estuary. At the same time, the model is most sensitive to the uncertainty in parameters related to deposition. Our results demonstrate that with the right measurements, making reliable estimates of estuary-to-sea export is possible. However, uncertainty in plastic transport processes, like deposition and remobilization, leads to poorly constrained parameters and increased overall model uncertainty. Automated sensors, targeted field experiments, and improved model structure can enhance export estimates and further improve understanding of plastic dynamics in estuaries.

1. Introduction

Plastic pollution in water bodies causes threats to aquatic organisms and human health (Chae and An, 2017; Al-Thawadi, 2020; Witczak et al., 2024; van Emmerik and Schwarz, 2020). Upon ingestion, microplastics can find their way into all tissues and internal organs (Witczak et al., 2024), where they can lead to metabolic, morphological and behavioral changes (Al-Thawadi, 2020). These microplastics (≤2.5 cm) have been degraded from macroplastic items (≥2.5 cm), like bottles. To mitigate the effects of aquatic plastic pollution, it is important to start at the source, and understand how macroplastics move through the global water system (Yadav et al., 2025). Estuaries are among the most dynamic and complex parts of the water system. Out of the 30 world's largest cities, 21 are located next to estuaries (Ashworth et al., 2015). As urban areas are large entry points for plastic pollution, this results in an increased plastic concentration in estuaries (Naidoo et al., 2015; Lucie et al., 2024). Anthropogenic pollution is difficult to predict, increasing the vulnerability of estuaries to its impacts. Estuaries are complex due to tidal forcing and freshwater–saltwater mixing, which periodically reverses flow direction and generates strong velocity shear and stratification (Friedrichs and Aubrey, 1988; Geyer and MacCready, 2013). Barotropic and baroclinic processes can generate plastic accumulation hotspots such as Estuarine Microplastic Maxima (Jalón-Rojas et al., 2024; Kaimathuruthy et al., 2026) and estuarine fronts (Wang et al., 2022; Kaimathuruthy et al., 2026), which promote particle trapping through convergence and stratification-driven dynamics.

To gain a better understanding of the behavior of plastic in rivers and estuaries, plastic observation techniques have been developed. These techniques include observation of plastic waste on riverbanks

* Corresponding author.
E-mail address: tim.vanemmerik@wur.nl (T.H.M. van Emmerik).

https://doi.org/10.1016/j.marpolbul.2026.119793
Received 23 February 2026; Received in revised form 20 April 2026; Accepted 21 April 2026
Available online 28 April 2026

during fieldwork (van Emmerik et al., 2020a), or by observing riverbank plastic from a boat Wilhelm et al. (2022). Plastic carried by the river can be observed visually on top of bridges (Schreyers et al., 2024b; van Emmerik et al., 2022), using cameras with AI (van Lieshout et al., 2020; Maharjan et al., 2022), using sonar (Boon et al., 2023), or nets to capture the plastic (Vriend et al., 2023). Moreover, flow paths can be captured using GPS trackers (Lotcheris et al., 2024; Tramoy et al., 2020). Such observations of plastic have demonstrated that plastic circulates in estuaries, as opposed to direct downstream transport towards the sea (Tramoy et al., 2020; López et al., 2021). The plastic is circulated by tidal dynamics (Schreyers et al., 2024b), wind-induced currents (Díez-Minguito et al., 2020), density-driven circulation (Defontaine et al., 2020) and vertical processes such as vertical mixing, settling and resuspension (Kaimathuruthy et al., 2026), and gets trapped in vegetation or anthropogenic structures (Gallitelli et al., 2024; Lotcheris et al., 2024). Moreover, cores of sediments in estuaries have shown that more recent deposited sediment layers contain an increasing amount of microplastics (Willis et al., 2017). This highlights the capability of estuaries to circulate and store plastic.

The circulation of plastic in estuaries contributes to the uncertainty of downstream plastic transport into the seas. To better understand the transport of plastic in estuaries, various modeling studies have been performed. These are either (1) process-based models (Cohen et al., 2019; Schernewski et al., 2021; Kaimathuruthy et al., 2025), to track plastic particle movements, or (2) mass-balance models that quantify import, export, and internal transport while conserving mass. The latter have been calculated using estuarine data averaged at a global scale (Biltcliff-Ward et al., 2022), or by focusing on a specific river section outside the estuarine zone (Schreyers et al., 2024a; Rosa et al., 2023). Mass-balance models for specific estuaries are already customary for different materials, like salt (MacCready et al., 2002), sediment (Maldegem et al., 1993), and nutrients (Nguyen et al., 2021), providing insight into transport dynamics in estuaries. Until now, an estuarine-specific mass-balance model for plastic transport has not been developed. Previous studies have shown that predicted transport of plastic into the seas does not match with the concentration in these seas (Roebroek et al., 2022). An estuarine-specific mass-balance model could decrease the uncertainty of estuary-to-sea transport by tracking plastic transport, and quantifying the amount that flows into the sea.

To increase the understanding of macroplastic (≥ 2.5 cm) transport from estuary to sea, we developed a tide-resolving (in contrast to tide-averaging) plastic mass-balance model for plastic transport, either floating or submerged, and retention in estuaries. The model was developed using knowledge from existing mass balances, estuarine-specific plastic measurements, and literature. The estuary is represented as a box, which includes storage terms, connected with fluxes representing the sources, sinks and pathways of plastic in an estuary. To make the model tide-resolving, we investigated the tide-related temporal patterns of plastic transport in the estuaries. The model is transferable and can be applied to any estuary, as long as river discharge and plastic transport data are available. In this study, we applied the model to two case studies: the Rhine–Meuse Estuary (RME) and the Saigon Estuary. With our paper we aim to develop and apply a transferable, tide-resolving mass-balance model to quantify macroplastic transport, retention, and export from estuaries to the sea.

2. Methods

2.1. Rhine-Meuse and Saigon field sites

2.1.1. Rhine-Meuse Estuary

The Rhine–Meuse Estuary (RME) is located in the West of the Netherlands, and is fed by the Meuse river and tributaries of the Rhine, namely the Lek and the Waal. The Meuse, Lek, and Waal rivers account for 14%, 16% and 70% of the river discharge, respectively (Schreyers et al., 2024a). The estuary has an open connection into the North Sea via the Nieuwe Waterweg and also discharges into the North Sea via the Haringvliet sluices. In between these waterways, a dense network of distributaries can be found. The combination of upstream river input, incoming tidal conditions at the Nieuwe Waterweg, and sluice operation at the Haringvliet, results in a complex hydrodynamic system. The average annual discharge at the Nieuwe Waterweg is 1674 m^3/s, and the tidal range is 1.76 m (Cox et al., 2021).

Therefore, the plastic mass balance was calculated for a smaller section of the RME. This section consists of parts of the Nieuwe and Oude Maas, and the Nieuwe Waterweg, debouching into the North Sea (Fig. 1b). It includes important parts of the estuary, such as the tidal influence from the estuary mouth and discharge from upstream rivers. Moreover, the Nieuwe Maas flows through the city of Rotterdam. This is the second largest city of the Netherlands, with 670 thousand inhabitants in 2024 (Rotterdam, 2024). It has been shown that plastic is more present in waters near cities (Naidoo et al., 2015). This also applies to the waters near the city of Rotterdam, having the highest floating plastic transport rate along the Rhine river (Kuizenga et al., 2023). The port of Rotterdam is located between the city of Rotterdam and the river mouth. This port is partly located at the banks of the study area. It is listed as number 11 of the biggest container ports in the world (Council, 2026), and transships 439 million tonnes of goods each year (Port of Rotterdam, 2025). Therefore, there is a potential of spillage from the port that can introduce plastic into the system. Overall, the study area effectively captures the variability of an urban estuary mouth.

2.1.2. Saigon Estuary

The Saigon–Dong Nai River estuary (from here Saigon) is located in the South of Vietnam (Fig. 1c). The 225 km river has its source in Cambodia, and drains a catchment area of 4717 km^2 (Camenen et al., 2020). The river flows through Ho Chi Minh City (HCMC), where multiple canals discharge the city's catchments into the river. The Saigon River flows into the Dong Nai River, which empties into the East Sea of Vietnam. The river is mainly driven by asymmetric semi-diurnal tidal flows, which makes the river even more complex. The discharge ranges from −2000 to 2000 m^3/s, and the tidal range is between −2 and 1.5 m (Camenen et al., 2020).

The plastic mass-balance model was applied to the 14 km downstream stretch of the Saigon River, as shown in Fig. 1d. This section was selected based on the available measurements. The upstream river boundary is the Thu Thiem Bridge, and the downstream river boundary is the outlet into the Dong Nai River. Therefore, the model area is located within the HCMC boundaries. The plastic inflow from HCMC into the river is large, with an input of 350 to 7270 grams of plastic per inhabitant each year, on a population of over 8 million people (Lahens et al., 2018). The amount of plastic is higher than for the RME, resulting in the ability to test the versatility of the model.

2.2. Mass-balance data acquisition

2.2.1. Rhine-Meuse Estuary

Data for the plastic mass balance of the section of the Rhine–Meuse Estuary (RME) were privately obtained from Rijkswaterstaat and Schone Rivieren. These data, combined with additional data from literature, are summarized in Table S1 under Rhine–Meuse Estuary data. The data includes modeled data of discharge and water level of the study area, and measurements of plastic on the riverbank, floating in the river, and in the water column. The plastic mass balance uses discharge data recorded and modeled in May 2022, which is in the snow-melt season of the Rhine, resulting in higher-than-average discharges. The first four data types in Table S1 (discharge, water level, and riverbank waste) contain data from the whole RME, and for the last two data types (floating and water column plastic) the locations are specified in Fig. 1b. Note that the water column plastic

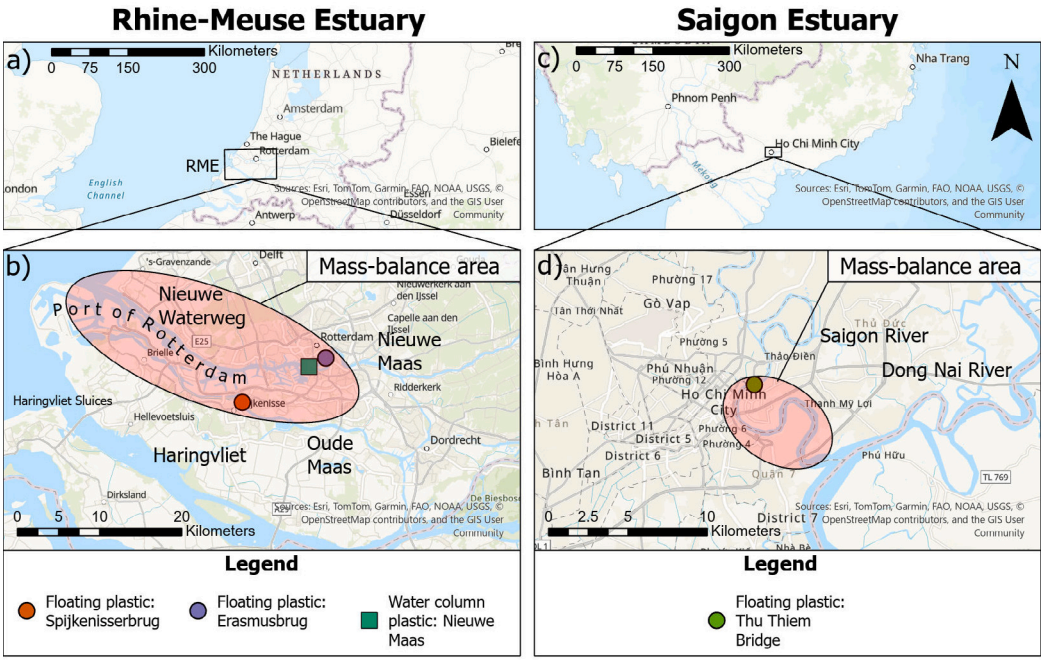

Fig. 1. Field sites. (a) RME with respect to the Netherlands. (b) RME. Outflow through the Nieuwe Waterweg and the Haringvliet. The red ellipse shows the area to which the plastic mass-balance model was applied. This includes the Nieuwe Waterweg, and parts of the Nieuwe Maas and the Oude Maas. The green box, orange circle, and purple circle indicate measurement locations of data used. (c) Saigon Estuary with respect to the South of Vietnam (d) Saigon Estuary in the Southern part of HCMC, including confluence with the Dong Nai. The red ellipse shows the area to which the plastic mass-balance model was applied. The orange circle indicates the Thu Thiem Bridge, where all measurements have been taken.

data was measured on a moving boat, and the measurement location is therefore an estimate. The discharge and water level data is modeled by Rijkswaterstaat in the modeling suite SOBEK. It simulates river conditions in the RME for 2534 different nodes. Discharge and water level data was selected from three nodes located at the model boundaries. Next to discharge and water level, the full dataset also contains salinity, water dispersion, water velocity, wind velocity, wind direction, and pressure difference, and is modeled for a year with 10-minute intervals. The plastic measurements done by Rijkswaterstaat are part of their macroplastic monitoring strategy (Rijkswaterstaat, 2025). These monitoring strategies have been developed and validated since 2021, and in 2024 the first annual measurement round was performed.

2.2.2. Saigon Estuary

Data for the plastic mass balance of the Saigon River were obtained from published hydrological and plastic pollution data in literature. These data are summarized in Table S1 under Saigon Estuary Data. The data types are similar to the data used for the RME plastic mass balance and include discharge, water level, riverbank waste, floating plastic, and water column plastic. Due to different measurement strategies, especially the frequency and duration of measurements differ. The data used for the model were recorded in May 2022. Since this is a wet month at the start of the wet season, this may potentially lead to higher than average water levels and flooding.

2.3. Conceptual plastic mass-balance model

Our plastic mass-balance model for estuaries is an adaptation of the river course model from Schreyers et al. (2024a) (Fig. 2). The adapted model consists of three domains: the river channel, left and right floodplain banks, and the area outside the river and floodplains. The model contains two storage terms: floodplain (S_{fl}) and river channel (S_c). The riverbanks are defined as part of the floodplains instead of the river channel. Plastic on riverbanks and floodplains can remain in place for longer periods of time, whereas plastic in river channels has a shorter retention time due to continuous water flow. Plastic can enter and leave the model domain via (1) external (outside of the river domain) input to the channel (i_c), (2) external removal from the channel (r_c), (3) external input to the floodplain (i_{fl}), (4) external removal from the floodplain (r_{fl}), (5) or via transport through the upstream and downstream river channel ($P_{c,river}$). Next to these terms providing transport between outside and inside the model domain, there is also a term accounting for the exchange of plastic between the two storage terms; $e_{fl,c}$ represents exchange between the floodplains and channel. The adapted model excludes transport of plastic between upstream and downstream floodplains, and the floodplain within the model, which is different from the model by Schreyers et al. (2024a). This was chosen based on the assumption that river transport is considerably higher than floodplain transport, especially when the length of the modeled river channel is long. Moreover, the adapted model also differs by assuming no relative transport differences between vertical water layers, and between the river channel and the river bed. Therefore, the river channel is not divided into a surface layer, suspended layer, and bed transport layer. These layers were not included due to insufficient data on plastic transport in these layers, and model simplicity.

The total storage of plastic within the model (S_t) is defined as the sum of the storage within the river channel (S_c) and floodplains (S_{fl}). Over time, the total storage changes, as its two containing storage terms change. This process is described in the equations below, using the transport terms shown in Fig. 2.

$$\frac{\Delta S_t}{\Delta t} = \frac{\Delta S_c}{\Delta t} + \frac{\Delta S_{fl}}{\Delta t} \tag{1}$$

$$\frac{\Delta S_c}{\Delta t} = P_{c,upstream} + i_c - P_{c,downstream} - r_c + e_{fl,c} \tag{2}$$

$$\frac{\Delta S_{fl}}{\Delta t} = i_{fl} - r_{fl} - e_{fl,c} \tag{3}$$

Some of the transport terms are bidirectional, making it possible to model tidal rivers: $P_{c,upstream}$ and $P_{c,downstream}$ are positive for transport

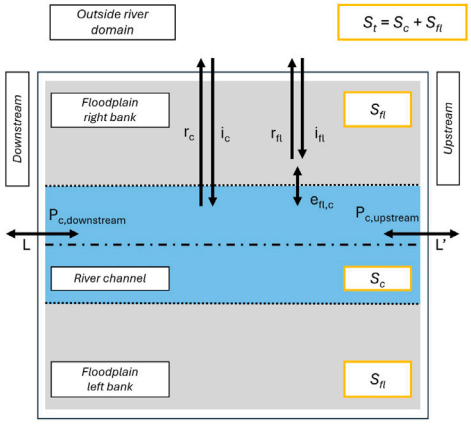

Symbol	Description
	Storage terms [kg]
S_t	Total river storage
S_c	Channel storage
S_{fl}	Floodplain storage
	Lateral transport terms [kg/timestep]
i_c	External input to river channel
r_c	Removal from river channel
i_{fl}	External input to floodplain
r_{fl}	Removal from floodplain
$e_{fl,c}$	Exchange from floodplain to river channel
	Longitudinal transport terms [kg/timestep]
$P_{c,upstream}$	Plastic transport at the upstream river boundary
$P_{c,downstream}$	Plastic transport at the downstream river boundary

Fig. 2. Conceptual estuary plastic mass balance in planform view, including nomenclature on the right.
Source: Adapted from Schreyers et al. (2024a).

in the downstream direction and negative in the upstream direction, and $e_{fl,c}$ is positive for transport from the floodplain storage to the channel storage. When combining Eqs. (2) and (3) into Eq. (1), the term $e_{fl,c}$ cancel because this is an internal exchange term. This results in the final equation for the total storage change:

$$\frac{\Delta S_t}{\Delta t} = P_{c,upstream} + i_c - P_{c,downstream} - r_c + i_{fl} - r_{fl} \quad (4)$$

2.4. Mass-balance model implementation

The model was implemented in R and is openly available through van Waterschoot et al. (2025). Depending on initial conditions, model preferences and available data, the model calculates storage and fluxes for the specified time period, where initial conditions represent the estimated legacy plastic present in the model at the start of the simulation. The following sections will explain how the river channel boundary transport (Section 2.4.1), exchange between river channel and floodplain (Section 2.4.2), and floodplain external input and removal (Section 2.4.3) have been implemented into the base model. This base model can be applied to any estuary as long as it has discharge, water level, and plastic transport measurements, such as described in Table S1. The model parameters chosen for the field sites in this study are described in Table S2. These parameters include, among others, initial conditions, boundary fluxes, discharge, water level, and river length. Moreover, Table S2 shows whether parameters need to be catchment-specific and if they are constants or timeseries.

Due to limited data availability for the Saigon estuary, only a 3-day simulation period could be applied to this model. To ensure comparability between both study areas, the same 3-day period was selected for the RME simulations. All simulations started on 01-05-2022 at 14:00. Because a more extensive dataset was available for the RME, an additional one-year simulation was also conducted for this estuary. This extended simulation was performed to assess whether differences existed between the results of the 3-day simulation and those of the one-year simulation.

2.4.1. River channel boundary transport

River channel boundary transport includes all the plastic in the river channels that cross the model boundaries, either floating or submerged. Depending on data availability, the model user has three options to quantify river channel boundary transport ($P_{c,river}$): (1) based on floating plastic transport measurements, (2) based on plastic concentration measurements, or (3) at the downstream boundary only, where the boundary transport is scaled to the amount of plastic stored in the river channel domain. For each model boundary, only one option can be selected. For the RME, all three options are available, while for the Saigon Estuary, only the first and third options were used.

Option 1 is the most direct way of quantifying the river channel boundary transport. Observed surface plastic transport is extrapolated to transport over the full water column, using a correction factor of 1.579 (calculated from Blondel and Buschman (2022)) for both the RME and the Saigon model. Note that this value is based on data from the Rhine, and we recommend using local correction factors if data are available. Since such local correction factor was not available for the Saigon Estuary, the correction factor of 1.579 was used. Continuous transport data can be applied as a time series; if only daily averages are available, observed values are assigned to each tide in a random order (positive during ebb, negative during flood) to simulate transport variability.

Option 2 multiplies modeled or measured discharges by a concentration. For the RME, depth-averaged concentrations from Blondel and Buschman (2022) were used. Similar to option 1, a concentration value is randomly selected at every turn of the tide.

Option 3 estimates river channel transport at the downstream boundary only. Here, plastic can leave but not re-enter the model, assuming immediate mixing of river plastic with the sea, and longshore transport away from the estuary. Transport is calculated by multiplying discharge by a concentration relative to the amount of river channel storage. This option assumes plastic takes a certain duration to travel through the model area. This duration is called the Transit Time, and is calculated as follows:

$$T_t = \frac{L_R}{d_T} \quad (5)$$

Where L_R is the river length in km, and d_T is the Net Daily Transport Distance in km/d. Therefore, the Transit Time (T_t) is in days.

The Net Daily Transport Distance accounts for hydrodynamic controls on plastic transport. This parameter was obtained from studies by Duncan et al. (2020) (1.0 and 0.7 km/d), Hauk et al. (2024) (0.2 km/d), Lotcheris et al. (2024) (2.0 km/d), and Tramoy et al. (2020) (2.3 km/d). Since the RME is not among these studies, an estimate was made by using the average of the Net Daily Transport Distances, giving each study the same weight. This results in a Net Daily Transport Distance of 1.3375 km/d. This first-order approximation neglects system-specific hydrodynamic variability but provides a practical baseline, with associated uncertainty quantified in following analyses. The study area in Lotcheris et al. (2024) is the Saigon Estuary, and therefore, the value of 2.0 km/d was chosen for the Saigon Estuary model.

The river length is defined as the distance between the upstream and downstream river channel boundary. For the Saigon Estuary, this is 14.1 km. The RME has multiple upstream river channel boundaries, so a weighted average length is calculated. The weighted average accounts for plastic transport: boundaries with higher plastic import are given more weight. This resulted in a river length of 27.82 km.

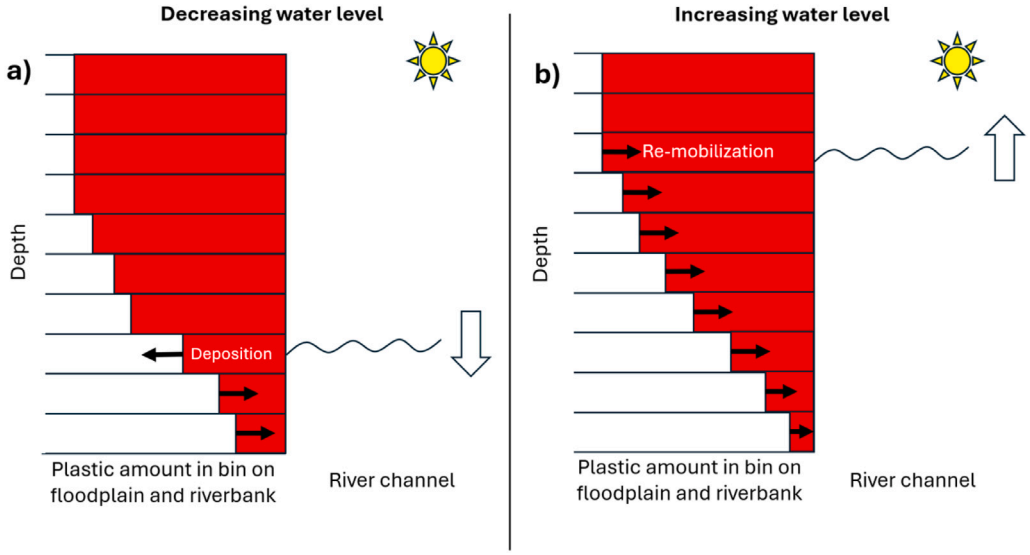

Fig. 3. Exchange process between river channel, and floodplain and riverbank storage ($e_{fl,c}$). The vertical bins contain a certain amount of plastic indicated by the red area. The amount of plastic is not limited, indicated by the opening on the left side of each bin. When there is an arrow within a bin pointing to the right (to the river), the amount of plastic in the bin is decreasing (remobilization). When there is an arrow pointing to the left (away from the river), the amount of plastic in the bin is increasing (deposition). (a) shows the scenario when the water level is decreasing, indicated by the downward pointing arrow, and (b) shows the scenario when the water level is increasing, indicated by the upward pointing arrow.

To make T_t inversely proportional to the discharge, the discharge values were corrected. From a one-year discharge timeseries, the median daily discharge was calculated. On a day with median discharge, plastic is transported across the downstream boundary at a speed that would empty the model storage in a time equal to the Transit Time. When the discharge is higher or lower, T_t is respectively lower or higher, inversely proportional to the amount of discharge.

For the Saigon Estuary, discharge measurements from the upstream Thu Thiem bridge were shifted in time as an estimation of discharge at the downstream boundary. Assuming the tide travels as a shallow water wave, the temporal shift can be calculated as follows:

$$\Delta t = \frac{\Delta x}{c} = \frac{\Delta x}{\sqrt{gh}} \tag{6}$$

where Δt is the time shift between high tide at both locations in s, Δx is the distance between both locations in m, c is the shallow water wave celerity in m/s, g is the gravitational acceleration in m/s^2 (9.81 m/s^2), and h is the water depth in m. This results in a time difference of 18.8 min. Since the available time series is in time steps of 5 min, the time series will be brought forward by 20 min.

2.4.2. Exchange between river channel and floodplain

The exchange of plastic between river channel storage and floodplain storage ($e_{fl,c}$) is guided by water level changes. Riverbank and floodplain plastics are stored in vertical, theoretical bins of 5 cm high spanning the range between the maximum and minimum recorded water levels in the available timeseries (Fig. 3). Plastic that is located in bins below the current water level is gradually released back into the river (3b). When the water level is decreasing, plastic from the river channel is deposited into the bin matching water level of that time step (3a). To account for the water level delay along the model domain, the water level in the middle of the river stretch was used. For the RME, this corresponds to the water level modeled at the river kilometer 1014 of the Nieuwe Waterweg (near the Geulhaven). For the Saigon Estuary, the water level recorded at the Thu Thiem Bridge was advanced by 10 min, based on the method presented in Section 2.4.1. This is half the delay presented in Section 2.4.1, since the distance Δt to the middle of the river stretch is also half of the distance between the upstream and downstream model boundary.

Whether plastic is deposited or remobilized is determined stochastically. When water levels decrease, a fraction of the river channel plastic becomes available for the stochastic simulation. This fraction is determined by the deposition-fraction parameter, which was calibrated based on experience and subsequently treated as a source of model uncertainty. The parameter was set to 0.05 for the RME, and 0.08 for the Saigon Estuary. Each available particle is assigned a random value between 0 and 1. Based on Lotcheris et al. (2024), all particles with values $\leq$ 0.97 will be deposited (General Deposition Probability, p_s). Particles with a value $\leq$ 0.07 are permanently deposited (Permanent Deposition Probability, $p_{s,permanent}$). The remaining plastic is temporarily deposited in the bins and becomes available for remobilization. All possible deposition mechanisms (e.g. lateral wind) are integrated in these Deposition Probabilities. For the remobilization process, the same procedure is followed. The Remobilization Probability, p_R, is 0.17, also based on Lotcheris et al. (2024). Since these probabilities all apply to a period of 1 h, they are converted to match the model time step, using Eq. (7):

$$p(\Delta t) = 1 - \exp\left(-\left(-\log(1 - p(1\text{ h}))\right) \cdot \frac{\Delta t}{60}\right) \tag{7}$$

Here, timestep Δt is in minutes, p(1 h) gives the probability of something occurring within 1 h, and p(timestep) gives the probability of something occurring within the timestep. As an example, the probability of 0.17 per hour equals 0.0306 per 10 min.

2.4.3. Floodplain external input and removal

We assumed that all external input and removal occurs via the floodplains (i_{fl} and r_{fl}), with no exchange between the outside river domain and the river channel ($i_c = 0$ and $r_c = 0$). All external input and removal (different from deposition and remobilization) is assumed to be human-induced, i.e., littering and cleaning of plastic. External input is divided linearly over all bins, with no plastic in the lowest bin and the most plastic in the highest bin. External removal of plastic is taken from the bins that are above the water level.

Floodplain external input of the RME was estimated using the dataset by Schone Rivieren, which followed the River-OSPAR method (van Emmerik et al., 2020a). To estimate riverbank littering, plastic measurements from sites inside and upstream of the model domain

were compared. Plastic found at upstream sites not located near urban areas or public areas is assumed to be deposited by the river alone. In contrast, plastic found at sites within the model domain is assumed to be the result of river transport and littering. Subtracting the average of both categories, and accounting for the measurement intervals and sampled riverbank lengths, results in a model-wide flux of 16.25 kg/hour of plastic littered on the riverbank and floodplains.

Floodplain external input of the Saigon Estuary was estimated from Lahens et al. (2018), which estimated a median plastic littering rate of 4.43 g per person per day in Ho Chi Minh City (HCMC). Scaling this value with the ratio of the river length within the model domain over the total river length within HCMC, resulted in a value of 539.0 kg/hour.

For the RME, floodplain external removal was based on the amount of plastic cleaned and the interval between Schone Rivieren cleanup efforts, resulting in a flux of 22.7 kg/hour. For the Saigon Estuary, only a single study by Nguyen and Bui (2023) was available to estimate floodplain external removal, resulting in a low flux of 3.5 kg/hour.

2.5. Export ratio, residence time, and delivery ratio

Three metrics were used to evaluate the model: the Export Ratio, the Residence Time, and the Delivery Ratio. The Export Ratio indicates how much of the incoming plastic is eventually exported downstream into the sea and is calculated as follows:

$$\text{Export Ratio} = \frac{\sum_{t=t_0}^{T} P_{\text{c,downstream}}(t)}{\sum_{t=t_0}^{T} P_{\text{incoming}}(t)} \tag{8}$$

Where t_0 is the first time step after the model spin-up period and T is the final time step of the simulation.

The Residence Time indicates how long the plastic resides in the model area before it leaves the model via the downstream export into the sea and is calculated as follows:

$$\text{Residence Time} = \frac{\frac{1}{N}\sum_{t=t_0}^{T} S_T(t)}{\frac{1}{N}\sum_{t=t_0}^{T} P_{\text{c,downstream}}(t)} \tag{9}$$

Where $S_t(t)$ is the plastic storage at time t, and N is the number of time steps in the averaging period. The result gives the Residence Time in time step units, which is then converted to days. The Residence Time should not be confused with the Transit Time mentioned in Section 2.4.1.

The Delivery Ratio was used to calculate the relative net transport of plastic across the river boundaries (Schreyers et al., 2024b), and quantifies the net transport relative to the total transport:

$$d_r = \frac{\overbrace{V_e - V_f}^{\text{Net transported plastic } (V_n)}}{\underbrace{V_e + V_f}_{\text{Total transported plastic } (V_t)}}. \tag{10}$$

Where V_e is the total amount of plastic transported during ebb, and V_f is the absolute value of the total amount of plastic transported during flood. Therefore, both V_e and V_f are positive.

2.6. Sensitivity analysis

To investigate which model parameters contribute most to model uncertainty, a Sobol' analysis was performed, which is a global, variance-based method. Input parameter values were sampled within their uncertainty ranges, and output variance is decomposed into individual parameters (first-order effects) and interactions among parameters (higher-order effects). For both the RME and the Saigon Estuary, the same parameters were evaluated: external input to floodplain storage (i_{fl}), external removal from floodplain storage (r_{fl}), Net Daily Transport Distance (d_T), deposition-fraction parameter (f_D), general probability of deposition (p_s), probability of permanent deposition ($p_{s,permanent}$) and probability of remobilization (p_R). The stochastic exchange between river channel and floodplain was replaced by fixed probabilities, to exclude randomness from the sensitivity analysis. A spin-up period was used: each parameter sample analysis was run twice over the same period, with the second run, used for the sensitivity analysis, starting from the last timestep of the first run.

The Sobol' sensitivity analysis was performed twice with 2000 base samples (18,000 parameter sets). The first used benchmark values (Table S2), with a range of +-10% to assess sensitivity to equal relative change in parameter values. The second used the full uncertainty range of the parameter values (Table S3), providing a more practical analysis reflecting real uncertainty of the parameter values. Some parameter ranges still have the +- 10% range when derived from literature or data.

In the RME, the Net Daily Transport Distance parameter used literature-based ranges. The Deposition Fraction, not based on either literature or data, was assumed very uncertain, receiving a range of one order of magnitude around the benchmark parameter value. For the general deposition probability ($\boldsymbol{p}_s$), a maximum value of 1 is chosen, since probabilities should not exceed 1. The external floodplain input ($\boldsymbol{i}_{fl}$) for the Saigon Estuary has a wider range, due to the uncertainty range being reported in Lahens et al. (2018). Moreover, the external floodplain removal ($\boldsymbol{r}_{fl}$) has a higher maximum range, due to likely underestimation caused by the lack of reports on cleaning efforts.

3. Results

This section presents the results of this study. The first three subsections eventually lead to the downstream export estimates presented in Section 3.4.

3.1. Channel and floodplain exchange results in the highest transport rates

For both the RME and the Saigon Estuary, plastic exchange between channel and floodplain storage ($e_{fl\text{-}c}$) results in the highest flux (Fig. 4a and e). For the RME, $e_{fl\text{-}c}$ in both directions is almost 60 tonnes during the three-day model run, 67 times larger than the total downstream export, the second largest flux. Similarly, in the Saigon Estuary $e_{fl\text{-}c}$ is 1300 tonnes, 22 times the total downstream export. These large magnitudes of $e_{fl\text{-}c}$, and the large channel and floodplain storage variations result from water level changes: when the water level decreases, floodplain storage increases, and vice versa (Fig. 4). The minimum floodplain storage occurs just after the maximum water level, when remobilization is still higher than deposition.

Globally, estuarine sediments and floodplains contain 2 to 10 times more plastic than estuarine water (Biltcliff-Ward et al., 2022). Moreover, Schreyers et al. (2024a) found that 98% of river plastics is stored in floodplains. This could suggest high channel–floodplain exchange, since large amounts of plastic are available for remobilization. However, neither study quantifies this exchange; Schreyers et al. (2024b) identified the uncertainty in channel–floodplain exchange as a need for further research. The method presented here, quantifying the exchange using water level, and the deposition and remobilization probabilities presented in Lotcheris et al. (2024), provide an appropriate first estimate for this uncertain transport term.

The distribution of plastic across floodplains and rivers in Fig. 4 falls in the range presented by Biltcliff-Ward et al. (2022), although the permanent floodplain storage remains very low in the short three-day simulation. A one-year simulation for the RME revealed that over a year, 83% of river plastic is stored in the floodplains and riverbanks (Figure S2 in the Appendix). This percentage is expected to increase towards the reported value of 98% in Schreyers et al. (2024a) when extending the model simulation to multiple years. For the Saigon Estuary, the percentage of plastic stored in the floodplains and riverbanks ranges between 60 and 92% during the three-day simulation. A long-term simulation was not possible due to a lack of discharge measurements.

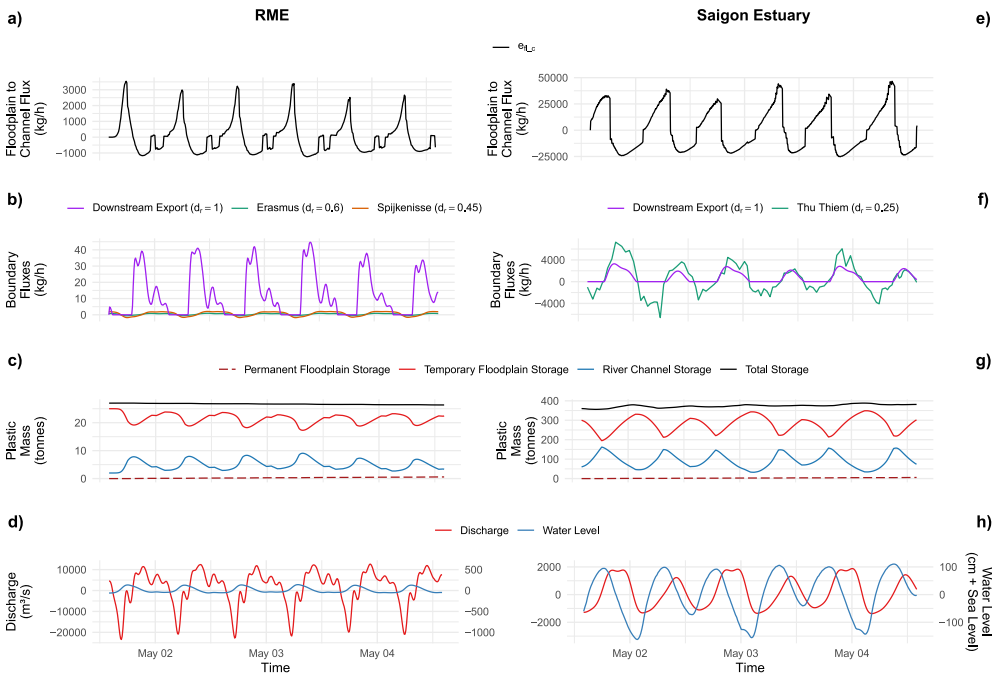

Fig. 4. Timeseries of a three-day model run, starting 01-05-2022 14:00. The left column shows the timeseries of the RME, and the right column the Saigon Estuary. Panels a and e show the flux of $e_{\text{fl-c}}$, which is the exchange from floodplain to river channel. Panels (b) and (f) show the river channel boundary fluxes in kg/h, where Erasmus is the upstream flux at the Erasmus bridge (RME), Spijkenisse is the upstream flux at the Spijkenisser bridge (RME), and Thu Thiem is the upstream flux at the Thu Thiem bridge (Saigon). Panels c and g show the storage terms in tonnes. The permanent storage starts at 0 at the beginning of the simulation and increases over time. Panels d and h show the discharge at the downstream boundary (left axis) and the water level (right axis). In the legend of panels b and f, the delivery ratio (d_r) is given for each river channel boundary. This ratio describes the relative net plastic transport and is derived from Schreyers et al. (2024b).

Since the channel and floodplain exchange results in the highest transport rates, it is expected that almost all plastic entering the model, either via the upstream river or due to anthropogenic littering, is deposited at least once on the riverbanks before being exported. For the RME, deposited plastic on the riverbanks is 267 times more than the total incoming plastic, while for the Saigon Estuary, it is only 16 times larger. This is in line with the study by Tramoy et al. (2020), who found a 100% deposit rate on tracked plastic bottles.

3.2. Higher absolute transport rates at the upstream model river boundary of the saigon estuary compared to the RME

The absolute and relative transport across the upstream river boundaries is larger for the Saigon Estuary than for the RME (Fig. 4, b and f). For the RME, the total storage stays fairly constant due to the small import at the upstream boundaries. However, Saigon Estuary shows clear total storage variations in line with the timescale of the tides because the import at the Thu Thiem Bridge is large enough to affect total storage. Overall, during the simulated period the net plastic transport at the upstream boundary in the Saigon Estuary (40,700 kg) is 600 times larger than the combined transport at both upstream boundaries in the RME (66 kg). The gross transport rates (absolute value of incoming and outgoing transport at the upstream boundary) is 1200 times larger for the Saigon Estuary (163,000 kg) than for the RME (135 kg). However, the average total storage of the Saigon Estuary is only 14 times larger than the RME, indicating stronger relative storage variability in the Saigon Estuary.

The delivery ratio d_r is 0.6 at the Erasmus Bridge and 0.45 at Spijkenisse (Fig. 4b), indicating higher net transport at the Erasmus Bridge than at Spijkenisse. In the Saigon Estuary, the net transport is even lower, with a d_r of 0.25 (Fig. 4f). Therefore, the downstream transport only slightly exceeds the upstream transport. This strong bidirectional transport across the boundary also contributes to the higher transport rates for the Saigon estuary than for the RME.

We explore two hypotheses for the higher upstream transport rates in the Saigon Estuary: (1) higher plastic concentrations, or (2) a larger range in flow velocity and discharge due to higher tidal amplitude. Plastic item concentrations are considerably larger in the Saigon Estuary (10-223#/m^3; Lahens et al., 2018) than in the RME (0.29-1.02#/m^3; Blondel and Buschman, 2022). However, the total volumes of water transported during the three-day modeling period for both rivers are of a similar order of magnitude (509 million m^3 for the Saigon Estuary and 821 million m^3 for the RME). For the second cause, the amount of water passing the bridges during the model simulation can be compared. For the RME, 227 million m^3 of water passes the Erasmusbrug, and for the Spijkenisserbrug, this is 594 million m^3. For the Saigon Estuary, this value is 509 million m^3. Therefore, values are around the same order of magnitude, and the higher upstream transport cannot be caused by the higher tidal amplitude. Therefore, the higher upstream transport in the Saigon Estuary can be primarily attributed to higher plastic concentrations.

3.3. Riverbank and floodplain plastic accumulate near the maximum water level limit

Fig. 5 shows the plastic distribution across the riverbank height over time for the RME and Saigon Estuary. Initially, plastic is evenly distributed above the initial water level. Plastic is mobilized when water levels increase and redeposited as water levels decrease. The amount of plastic deposited depends on the channel's plastic storage. Over time, a pattern emerges where plastic accumulates mainly at higher elevations, while lower, more frequently submerged bins, contain less plastic. The horizontal, lighter strikes occur when the water level drops rapidly, limiting time for plastic to deposit. In contrast, when the water level remains fairly constant for a longer time, more plastic can be deposited (see for example around -30 cm in Fig. 5b).

The increase in plastic with riverbank height is caused by the water level rarely and only briefly submerging these elevations, as can be seen

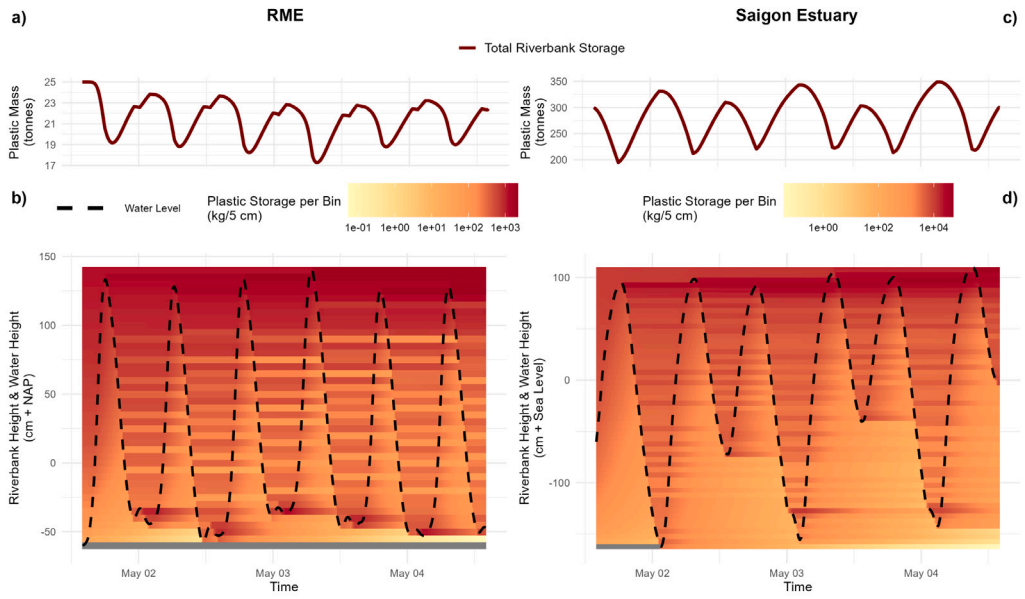

Fig. 5. Heatmap of the riverbank plastic storage of a three-day model run, starting 01-05-2022 14:00. The left column shows the timeseries of the RME, and the right column the Saigon Estuary. Panels a and c show the total riverbank storage in tonnes. Panels b and d show the plastic storage per bin in kg/5 cm, for different heights and over time. Note that the scale of the plastic storage per bin is logarithmic. The water level is also shown by the dashed black line. The unit on the *y*-axis for panels b and d is cm above sea level, where the Amsterdam Ordnance Datum (NAP) is used for panel b.

by the higher elevations of the water level lines in Fig. 5 b and d. Plastic continues to accumulate due to anthropogenic littering (i_{fl}), which is distributed over the exposed riverbank bins. Occasional flooding causes brief remobilization, followed by deposition, further increasing storage near the highest elevations. At the end of the year, the storage is higher than when i_{fl} would have been the only factor of storage increase (see also Figure S1, showing the seven highest riverbank storage bins during the one-year RME simulation). Targeting these higher elevations of the riverbank could therefore contribute to effectively removing plastic during clean-up efforts.

Our results provide new insights on the deposition along and onto the riverbank. Tasseron et al. (2024) investigated the distribution of plastic along the riverbanks, and found that 37.5% of the locations showed a deposition line parallel to the waterline, consistent with the modeled accumulation at higher elevations. The remaining sites showed clustered or random distributions, which cannot be seen in Fig. 5. Similarly, Grosfeld et al. (2024) found that plastic is deposited on floodmarks, after which it is pushed towards the higher elevations when the water level rises. This is in line with what can be seen in Fig. 5. The difference between the process described by Grosfeld et al. (2024) and the movement of plastic in this study is that the plastic is not pushed, but remobilized and deposited at a higher elevation.

3.4. Estuary-to-sea export promoted by the parallel fluctuations of water level and discharge in tides

Estuary-to-sea export (Downstream Transport) varies with tide dominated discharge and channel storage. The positive (downstream) discharge coincides with the maxima in channel storage (Fig. 4). During the three-day simulations, average daily export was 290 kg for the RME and 19,431 kg for the Saigon Estuary, which, if extrapolated, would correspond to 106 tonnes/year and 7092 tonnes/year, respectively. When using the full-year model run presented (Figure S2), the yearly downstream export becomes 13.3 tonnes for the RME. This is an order of magnitude smaller than extrapolated from the daily transport, due to a higher net discharge and overestimated initial conditions for the three-day simulation. The Export Ratio is 3.97 for the RME and 0.73 for the Saigon Estuary. This means that for the Saigon Estuary, an amount equal to 73% of the incoming amount of plastic is exported during the simulation, while 27% is stored within the estuary, mostly on the riverbanks and floodplains. However, the RME exports a surplus of plastic during this period, which is 3 times as large as the incoming plastic. This higher export has the same cause as explained for the higher yearly downstream export for the three-day simulation.

Since export is the product of discharge and channel storage, estuary-to-sea export peaks when high water levels coincide with high downstream discharge (Fig. 4, b and d). In the Saigon estuary (Fig. 4, f and h), export occurs just after the channel storage peak. Therefore, the export could have been higher if the peaks in water level and discharge aligned more closely. However, when the discharge and water level are out of phase, estuary-to-sea export would be suppressed. Thus, the interaction between water level and discharge strongly influences estuary-to-sea export predictions. The location of the water level measurements along the model domain also plays an important role: for long river stretches, the time shift between upstream and downstream water level peaks may be up to several hours. This can result in the water level being even more in phase with the discharge variation, resulting in higher estuary-to-sea export.

Next to the effect of synchronous water level and discharge, a stronger tide could also enhance export in the model, as particles leaving the domain are not allowed to re-enter. A larger tidal range increases downstream discharge at the outlet and thus plastic export. However, when the tidal range is larger, but does not change, it does not necessarily contribute to more plastic remobilization. The amount of plastic determines how much plastic is remobilized during high water levels. The amount of plastic on the riverbanks does not increase when the water levels have a constant larger range because the deposition of plastic is determined each timestep, for the bin at the current water level. A larger water level range would result in more spread out plastic and therefore not increase the amount of riverbank plastic and remobilization. On the contrary, when the tidal range increases during moments of the year, due to spring-neap cycles, storm surges or extreme discharge (Amaral et al., 2023), plastic deposited at the previous maximum water level limit will be submerged more often, resulting in higher plastic remobilization. So, stronger tides could increase export in terms of discharge, and water level. This

theory could be tested with two catchments that have similar plastic content, but stronger tides. Potentially, the downstream discharge of the RME could be increased, and the results compared with the original simulation. van Emmerik et al. (2018) used a combination of counting, sampling, mathematical relations with hydrology, and extrapolation to estimate the plastic estuary-to-sea export for the Saigon Estuary. Their estimate resulted in a downstream export of 7500–13,700 t/y for the Saigon Estuary. The export of 7092 tonnes is just short of this range, but definitely in the same order of magnitude. The fact that two different studies result in the same export estimate supports the reliability of these results.

For the RME, the model estimated an estuary-to-sea export of 106 t/y. No direct estimates exist for the RME, but van Emmerik et al. (2022) estimated the floating plastic mass transport of the upstream rivers towards the river mouth. Converting surface transport to total water column using the conversion term of 1.579 (see Section 2.4.1) results in mean values of 25.3-92.8 t/y for the Rhine, and 24.2-71.8 t/y for the Meuse, with median values of 2.1–9.9 t/y and 1.9–10.1 t/y respectively. Therefore, RME export from this study falls within the combined range of median values.

In the one-year simulation for the RME (Figure S2), the estuary-to-sea export is much lower: 13.3 t/y, which still falls within the range of mean estimates of van Emmerik et al. (2022). The discrepancy between the three-day and one-year model simulations is caused by the extrapolation of the three-day model: the three-day period had a 10.5% higher average positive discharge than the one-year average. Moreover, an overestimation of the initial conditions can result in higher river channel storage, and thus higher export values, an effect that smoothens out over a one-year model run. Overall, the modeled export falls within the range of previously reported literature, supporting the reliability of the model.

The high export ratio values mentioned here imply that the spin-up time for the three-day simulations is not large enough. Combined with an overestimation of the initial floodplain storage, this results in an imbalance in short simulations. For the one-year simulation (Figure S2), the Export Ratio is 0.51, indicating that the model has stabilized and is not exporting more plastic than it is receiving. Comparing total estuary-to-sea export to annual deposition on riverbanks and floodplains (including repeated deposition due to remobilization), the export is 12500 times smaller than the total magnitude of the deposition flux. This supports the findings in Section 2.4.2, confirming that deposition and remobilization play a big role in determining plastic export in estuaries.

3.5. Deposition fraction and general deposition probability cause the highest model uncertainty

Fig. 6 shows the results of the Sobol' sensitivity analysis for both the 10 percent and full uncertainty parameter range (see Section 2.6). The Sobol' sensitivity index values should range between 0 and 1, and the total-order value of a certain parameter should be higher than or equal to the first-order value, since the total-order value also adds the interactions with other input parameters. Only when there is no interaction with other parameters, both values are equal.

Figs. 6a and b show some confidence intervals are larger than 1, or smaller than 0. This behavior can have multiple causes: (1) the relation between input and output is noisy, (2) underestimation of the total output variance, or (3) strong parameter interactions, resulting in overlapping contributions. Additionally, the sensitivity of the Deposition Fraction (f_D) on the Export Ratio parameter uncertainty for the RME shows a lower value for the total-order index than for the first-order index. This also occurs for the sensitivity of General Deposition Probability (p_s) on the Residence Time 10% range for the RME. However, since the confidence intervals are large, it is still possible that the total-order index is higher than the first-order index.

For the 10 percent parameter range, the model is most sensitive to the General Deposition Probability p_s (Fig. 6a and b). For both the Export Ratio and the Residence Time, in both estuaries, the Sobol' index value is the highest; p_s also shows the largest confidence interval. This indicates that a change in the parameter did not always result in the same change in model outcome. Even its minimum value of the first-order index is higher than any of the maximum first-order index values of other parameters. In contrast, the external removal from floodplain storage (r_{fl}) and probability of permanent deposition ($p_{s,permanent}$) have negligible effect in all simulations, while the remaining parameters show little sensitivity and little difference between the estuaries and model outputs.

When looking at the full uncertainty ranges, different parameters cause the highest model uncertainty (Fig. 6c and d). For the Export Ratio, f_D has the highest index values, for both the RME and the Saigon Estuary. For the RME, the Net Daily Transport Distance (d_T) is also higher than the other parameters. For the Saigon Estuary, this is the case for external input to floodplain storage (i_{fl}), especially the total-order index values are higher. For the Residence Time, the Deposition Fraction still shows high index values for both the RME and Saigon Estuary, except for the first-order value of the RME. For the RME, the Net Daily Transport Distance index value and p_s also show higher values than the rest. For the Saigon Estuary, this is only the case for p_s. The remaining parameters show no sensitivity.

The high sensitivity to the General Deposition Probability (p_s) could be explained by the high channel–floodplain exchange rates. The deposition probability directly impacts the plastic deposition, and thus indirectly the remobilization. Therefore, $p_{s,permanent}$ and p_R are dependent on the general amount of plastic deposited p_s, and show lower sensitivities. A high sensitivity to the Deposition Fraction (f_D) would be expected, since this parameter determines deposition together with p_s. However, this is not the case, indicating a higher sensitivity to the probability of deposition, then to the amount of plastic selected for the probability calculation. Since f_D has never been estimated before, it received a high parameter uncertainty range (Table S3), resulting in a high sensitivity to this parameter (Fig. 6c and d).

The Net Daily Transport Distance (d_T) for the Saigon Estuary has been estimated (Duncan et al., 2020; Hauk et al., 2024; Lotcheris et al., 2024; Tramoy et al., 2020), and therefore the parameter uncertainty range was only 10%. However, d_T was never estimated for the RME. Therefore, the uncertainty range was set to the range found in other estuaries, as described in Section 2.4.1. This results in a larger sensitivity for the RME compared to the Saigon Estuary. Since the calculation of the Residence Time is more directly related to the amount of plastic leaving the model (S_T and $P_{c,downstream}$) than the Export Ratio ($P_{c,downstream}$ and $P_{incoming}$), the sensitivity is higher for the Residence Time.

i_{fl} shows higher index values for the Saigon Estuary than for the RME (Fig. 6c). This is due to the larger parameter uncertainty for the Saigon Estuary compared to the RME. For the RME, the range is 10%, but for the Saigon Estuary it ranges from −78% to +349%, as taken from Lahens et al. (2018). Moreover, the total-order index value is higher, indicating that i_{fl} especially influences the output in combination with other parameters. In contrast to the Export Ratio, the Residence Time is not sensitive to the range of i_{fl}. This can be explained by the direct influence on the number of plastic inflow into the model, which is used in the calculation for the Export Ratio, but not for the Residence Time. The reverse can be said for p_s when comparing between Fig. 6(c) and (d). This parameter does not influence inflow or outflow directly, but it does impact the total storage by depositing more or less plastic on the riverbanks.

4. Discussion

4.1. Exchange between river channel and floodplain

The method to simulate deposition and remobilization used in this paper is not completely in line with the results in literature. Grosfeld

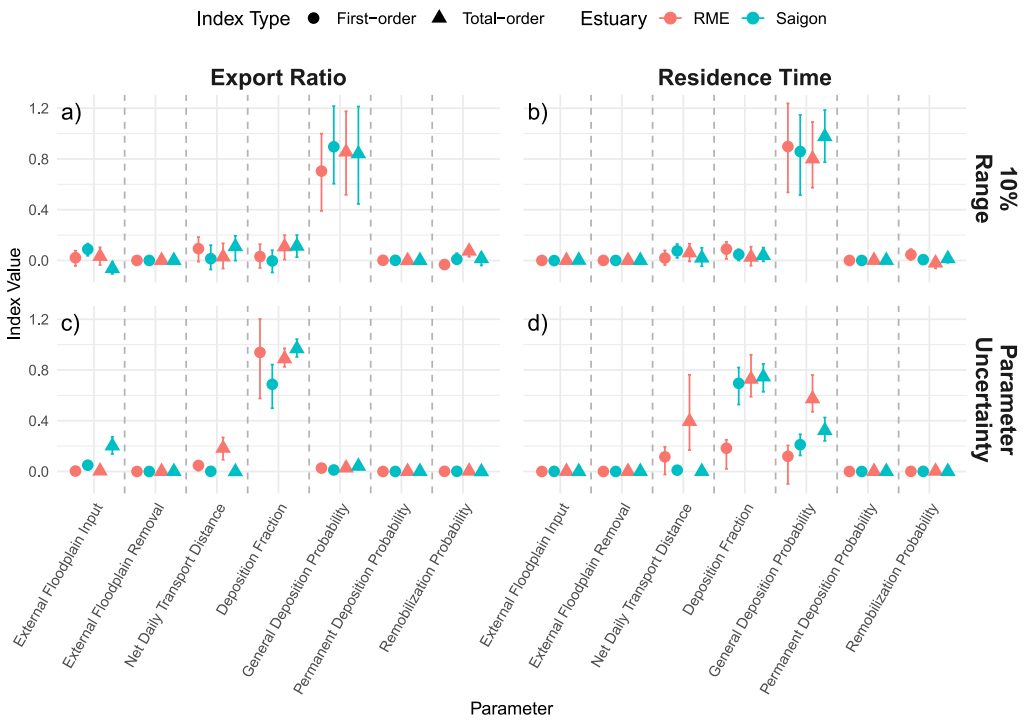

Fig. 6. Sobol' sensitivity indices. The top row shows the results with a parameter range of +−10%, where (a) shows the parameter effect on the Export Ratio, and (b) shows the parameter effect on the Residence Time. The bottom row shows the results according to the parameter uncertainty, where (c) shows the parameter effect on the Export Ratio, and (d) shows the parameter effect on the Residence Time. First-order and Total-order indices are shown for both the RME and the Saigon Estuary.

et al. (2024) concluded that remobilization occurs during water level rise, but also increases when the water rises faster. In our model, remobilization occurs per timestep when the riverbank is flooded. When a higher portion of the riverbank is flooded, remobilization is higher due to remobilization occurring in more bins. Moreover, Climo et al. (2022) found that waves induced by inland navigation significantly increase remobilization of riverbank plastic. Such inland navigation induced waves were not included in the model. Besides remobilization, Grosfeld et al. (2024) found that the deposition rate is almost constant. In the model, deposition only occurs during a decrease in water level. Therefore, we recommend future model adaptations to better represent the results of literature. Moreover, the current model only used deposition and remobilization probabilities from the GPS-tracker study by Lotcheris et al. (2024). To improve, outcomes of different GPS-tracker studies (Tramoy et al., 2020; Ledieu et al., 2022) can be used to potentially disconnect deposition and remobilization from water level variation, and base it solely on observations. However, experimenting with the coupling between water level variation and floodplain deposition and remobilization also resulted in useful results. In the end, both the results of this study and the study by Grosfeld et al. (2024) show the accumulation of plastic at higher elevations.

To further improve the representation of the plastic exchange between river channel and floodplain, we recommend decreasing the uncertainty of parameters related to this exchange, as described in Section 3.5. Those parameters are General Deposition Probability (P_s), the Net Daily Transport Distance (d_T), and the Deposition Fraction (f_D). All these parameters are related, since they describe the deposition and remobilization process of plastic. For the Saigon Estuary, the uncertainty of the parameters was lower, since there have already been studies to estimate their processes. These studies can also be applied to the RME. For example, GPS trackers or Lagrangian models can be used to follow the plastic trajectories. Lagrangian models, similar to the on presented in Queiroz et al. (2026), have not been applied to both the RME and Saigon yet. GPS experiments were already performed for the Ganges (Duncan et al., 2020), the Seine (Tramoy et al., 2020), and the Saigon, similar to this study (Lotcheris et al., 2024). Since these studies did not focus on the most downstream area of the estuaries, such experiments at the downstream end of the RME could result in new findings regarding plastic movement near the outlet to sea, and potentially into the sea. Regarding the model, such an experiment could help with increasing the accuracy of d_T by following the trajectories of the plastic. Moreover, the estimates of P_s and f_D could also benefit from such a study, since the probability and frequency of deposition can be calculated, which are both related to these parameters. Another example could be to distribute plastic items across the riverbank at different heights (preferably items that were already located on the riverbank by deposition), and observe whether they remobilize upon a change of water level. A similar study was performed by Climo et al. (2022) to capture the impact of waves from inland navigation on the remobilization of plastic. These waves cause changes in the riverbank water level, similar to the change in water level due to tides. Finally, deposition and remobilization could be studied using a physical scale model in a laboratory. This would include modeling an estuary, and simulating plastic transport in a controlled environment. Such scale studies have already been performed for other purposes. Osei-Twumasi et al. (2014) modeled a complete estuary to study hydrodynamic and solute transport processes, and De Ruijsscher (2016) constructed a scale model of a river channel to study the effect of longitudinal training dams. Even though the transport mechanics in such a model study might be different than in a large estuary, it could be valuable for hypothesis generation for other studies.

4.2. Large model area

The model has a large model area, with just one box for the river channel storage and one for the floodplain storage. This means that long river channel stretches of the model area (31 km in the RME and 14 km in the Saigon Estuary) are treated as spatially uniform. This overlooks the different rates of plastic transport and storage along the estuary. Additionally, the amount of plastic leaving the estuary is

calculated using the Net Daily Transport Distance and the river length (Eq. (5)). However, plastic is circulated in estuaries (Schreyers et al., 2024b; Díez-Minguito et al., 2020) and their storage may be greater either within the main estuary or in upstream river sections depending on the specific hydrodynamic characteristics of the system, while also varying with external forcing. For example, in the Gironde estuary, plastic accumulates in the tidal rivers during dry periods while they are pushed downstream in wet periods (Kaimathuruthy et al., 2026). This indicates that the Net Daily Transport Distance decreases towards the downstream river boundary, closer to the sea. Therefore, the current approach may overestimate the plastic outflow. Moreover, due to the large model area, there is no delay between remobilization, reaching the downstream model boundary, and the resulting export. This also supports overestimation of plastic outflow. We recommend improving the model by dividing the estuary into multiple boxes. For our plastic mass-balance model, the transport between boxes could be calculated based on discharge and concentration of the boxes, while the plastic outflow could be determined using the Net Daily Transport Distance specific to the most downstream section. This would then result in a more accurate representation of the plastic export to sea, and prevent the model from immediately exporting plastic that has just come in from the far upstream model boundary. Moreover, when multiple boxes are used, the size of the study area can be increased to include the full estuary. This allows for better comparison between estuaries.

4.3. Application of data to the model

The data that needs to be supplied to the model is very specific. As a minimum, discharge, water level, and either plastic transport measurement from bridges or plastic concentration are needed to run a simulation. Moreover, this data should be continuous and with the same measurement interval. Some of the data encountered in this study are measured during a small part of the day, like data from van Emmerik et al. (2019, 2022), and bridge plastic transport measurements from Rijkswaterstaat. To simulate a period using daily averaged data, observed fluxes were assigned in a random order. However, this randomization results in changing boundary fluxes between simulations and affects the calculation of the delivery ratio, which introduces additional uncertainty. Moreover, there is often a lack of discharge data. For the RME, modeled data were available for the whole study area, which provided the opportunity to select appropriate river model boundaries. However, for the Saigon Estuary, only a single continuous discharge dataset was available for the selected upstream river boundary. To apply discharge data at the downstream river boundary, the data were then shifted in time to account for the tidal delay, adding uncertainty to the simulation. Numerical hydrodynamic or particle-transport models may also help optimize the simulations in other ways, for example by guiding a more physically consistent temporal distribution of boundary fluxes.

In an ideal world, there would be data for all estuaries, and all data would be formatted the same way. To get as close as possible to this ideal situation, we recommend measurement procedures and the resulting data file formatting to be standardized. Standardization already occurs for riverbank measurements following the OSPAR protocol (van Emmerik et al., 2020a). However, the resulting data is not always formatted similarly, resulting in different dataset structures. This leads to difficulties in comparing data and applying data to analyses. There are examples of existing efforts to make standardized data reporting formats. An example is the FAIR principle to publish Earth and environmental science data (Crystal-Ornelas et al., 2022). This principle aims to make data more accessible and reusable by providing guidelines that communities can use to create new data formats. Moreover, there are existing software modules that can help with assigning metadata and the creation of datasets, to comply with data standards (Jones et al., 2023). Potentially, these principles and tools can be applied to report plastic measurements in hydrology.

4.4. Sensitivity analysis

The Sobol' sensitivity analysis revealed some unusual values for the calculated indices. This includes wide confidence intervals, indices greater than 1, and parameters where first-order indices were smaller than total-order indices. This suggests strong interactions between parameters or structural noise and instability in the model. To improve the reliability of the sensitivity analysis, we recommend the model equations to be revised to reduce noise, the number of model evaluations to be increased to narrow confidence intervals, and alternative sensitivity methods to be explored aiming to be less sensitive to model nonlinearity and interactions. To reduce noise, a method by Prikhodko and Kotlyarov (2018) could be used that performs noise correction to improve Sobol' index estimation. Moreover, the Sobol' analysis could be used to further test parameter interactions. There is a constant feedback loop between the amount of plastic deposited and remobilized. Therefore, especially the parameters that are involved in this process are expected to show strong parameter interactions. The strongest parameter interactions are expected for the deposition-fraction parameter (f_D) and the general probability of deposition (p_s), since these are multiplied to calculate the deposition.

4.5. Future measurement recommendations

We recommend further observations to focus on quantifying the effect of tidal range on the net plastic transport and delivery ratio. This allows to compare average behavior of rivers with varying mean tidal range, to better understand where around the world plastic is most likely to be exported into the ocean. Furthermore, this sheds light on the temporal variation of net transport for specific rivers and whether tidal range promotes or attenuates plastic export into the sea.

The amount of external input of plastic on the riverbanks was calculated using observations of the increase in riverbank plastic after each measurement and cleaning event of Schone Rivieren. Most of the time, months passed between two of these measurements, during which the hydrologic conditions can impact the amount of plastic on the riverbanks. Especially in urban environments, it is unknown which plastic has an anthropogenic origin and which is deposited. To better determine external input of plastic, the method used by Grosfeld et al. (2024) can be used to observe the change in plastic on an urban riverbank over time. The riverbank should be observed with a time interval of at most a day, to remove the impact of tidal water level change. In combination with water level data, this may also give a better understanding of the deposition and remobilization process. Moreover, disintegration of plastic, something that was not included in this study, could be quantified using this measurement strategy.

Besides focusing on the most sensitive parameters, increasing the general data availability in estuaries could result in longer model simulations. The available plastic transport measurements from bridges only covered a few days, for both the RME (Vriend et al., 2020) and the Saigon Estuary (Schreyers et al., 2024b). Therefore, for the Saigon Estuary, only 3 days could be simulated. For the RME, the lack of data meant that the average concentration in combination with discharge had to be used. To increase the observations of floating plastic across bridges, cameras could be used to observe the river and plastic flow during daylight. Afterwards, the images can be evaluated using a deep learning algorithm to count the plastic and calculate the transport rate. A similar method was used by van Emmerik et al. (2025), who used this method to quantify the relation between water hyacinth coverage and plastic concentration. Moreover, van Lieshout et al. (2020) used a similar technique, which is expected to be more reliable than human monitoring. Therefore, they have already shown that using cameras to detect plastic is possible, and with the constant improvement of technology, future measurement campaigns using cameras could be able to consistently measure plastic transport during daylight. Besides using cameras to measure floating plastic, suspended macroplastic can

be detected using the echo from an Acoustic Doppler Current Profiler (ADCP). This has been demonstrated by Boon et al. (2023), who showed that when the ADCP data is calibrated, plastic transport can be estimated in the correct order of magnitude. However, more research (e.g. on the echo of items and the sensitivity of the calibration) is needed to produce continuous suspended plastic transport data.

Previous work has demonstrated that vegetation and artificial structures can effectively trap plastics in rivers and estuaries. Examples include the trapping of plastics in floating vegetation and mangroves (Lotcheris et al., 2024; Hauk et al., 2026), the retention of plastics on floodplain vegetation and structures after floods (Vriend et al., 2020), and collection by clean-up technology . Their impact on the estuarine plastic mass balance remains unclear, and were therefore recommend future measurement efforts to also quantify plastic retention and remobilization in vegetation and artificial structures.

Lastly, an important assumption of the model is the unidirectional transport at the downstream boundary. Plastic can only leave the model here, and not enter, due to the assumption described in Section 2.4.1. However, investigating this could provide important insights into estuarine plastic transport. This could be done by using nets to capture plastic, as was already performed by Blondel and Buschman (2022) and Vriend et al. (2023). When applying this method at the boundary between the estuary and the sea, the assumption of unidirectional transport at the downstream boundary could be tested. To assess the unidirectional transport in future model development, an additional near-shore storage box could be added. This box could serve as a short-term memory for plastic export, being able to reintroduce exported plastic from the sea during flood tide.

5. Conclusion

This study developed the first plastic mass-balance model that can be applied to tidal estuaries. The resulting model opens new perspectives to understand the physical processes ongoing in estuarine systems by coupling stochastic plastic deposition and remobilization processes with a simple tide drive hydrodynamic model. The model was successfully applied to the Rhine–Meuse Estuary (RME) and the Saigon Estuary.

Model development demonstrated that the main plastic fluxes, such as riverbank-to-channel exchange, upstream plastic river transport, and external fluxes, can be estimated using field measurements, literature-based parameters, and simplification of processes, such as the exchange between river channel and floodplain (Section 2.4.2). Moreover, an estimate of estuary-to-sea export can already be made using only discharge, water level, and plastic concentration measurements.

Absolute plastic river transport (in both upstream and downstream directions) at the upstream model river boundary is much higher for the Saigon Estuary than for the RME. The magnitude of the combined transport rates in both directions is 1200 times larger for the Saigon Estuary than for the RME. This difference is mostly caused by higher plastic concentration in the Saigon River. However, the relative net transport is lower for the Saigon Estuary, with a delivery ratio of 0.25, where this is 0.6 and 0.45 for the Erasmusbrug and Spijkenisserbrug, respectively, indicating less effective transport for the Saigon Estuary. This shows that there can be large differences in transport dynamics in the upstream parts of estuaries, and research is needed to further study its impact on plastic storage and export.

The model analysis of the RME and Saigon Estuary revealed a unique connection between discharge and water level that has never been found before. The timing between discharge and water level has proven to be an important factor in the amount of plastic exported to the sea. Under normal conditions, the tides promote the export of plastic to the sea. When maxima in water level and discharge coincide, more plastic is remobilized and available in the channel, and eventually exported to the sea. The reverse is true when minima in water level coincide with maxima in discharge. Therefore, the location of measurements for the model should be carefully selected to avoid impact on the model results, due to the lag time experienced because of tides. Further research could indicate whether this also occurs in other estuaries. This finding could improve estimations of plastic export from estuary to sea.

The estuary-to-sea plastic export was estimated to be 19,431 kg/d for the Saigon Estuary. For the RME, the export was estimated to be 290 kg/d based on the three-day simulation, and 13.3 t/y based on the non-extrapolated one-year simulation. The export estimates for the RME fall within the uncertainty range of previous estimates. For the Saigon Estuary, estimates from previous studies do not exist. Since the export estimates are in line with previous studies, applying the mass-balance model to estuaries that already have estimates of export could further test the versatility and accuracy of the model.

Model simulations confirm that most of the plastic is stored in the floodplains and on the riverbanks, with 83% of the plastic in the RME stored there after one year. Besides, deposition and remobilization resulted in the largest model fluxes, with magnitudes of 20 t/d for the RME and 430 t/d for the Saigon Estuary. Over time, deposited plastic accumulates near the maximum water levels of the tides. These maximum water levels are determined by the maximums reported in the water level data. Since the data length is one year, the return period of the maximums should be one year, or shorter when this level is reached more often. The amount of plastic on the riverbanks decreases when getting closer to the river (towards lower elevations of the riverbank). Previous studies found a similar trend for non-tidal rivers, but there, the plastic is pushed towards the higher elevations when the water level rises, instead of constant remobilization and deposition. These results indicate that plastic deposition and remobilization play a very important role in estuaries.

A similar conclusion was found from the sensitivity analysis. Per percentage change of the parameters, the model is most sensitive to the General Deposition Probability (p_s). When taking into account the uncertainty of the estimated parameters, the Deposition Fraction (f_D) causes the highest uncertainty for the Export Ratio, while a combination of f_D, p_s, and the Net Daily Transport Distance (d_T) cause the highest uncertainty for the Residence Time. Together with the findings from the previous paragraph, and because its current understanding is low, deposition and remobilization would be one of the most important topics to study to increase understanding of plastic in estuaries. This would result in more accurate predictions and a more reliable model.

Concluding, this study presents a novel mass-balance model that can be applied to any estuary to better understand plastic dynamics, as long as the required data is available (Table S2). The model is able to produce reliable estuary-to-sea plastic export estimates that are in line with previous studies. Looking forward, the model and its predicting ability can be strengthened through long-term measurement campaigns using automated sensors, specific field experiments, and the development of multi-box model frameworks to improve spatial accuracy. By continuously narrowing knowledge gaps, uncertainty in plastic budgets and exports can be reduced, aiding strategies that aim to decrease plastic pollution in the environment.

CRediT authorship contribution statement

D.M.P. van Waterschoot: Writing – original draft, Visualization, Validation, Software, Project administration, Methodology, Investigation, Formal analysis, Data curation, Conceptualization. **S.A.J. Tas:** Writing – review & editing, Supervision, Project administration, Conceptualization. **N. Gratiot:** Writing – review & editing, Validation. **P. Vriend:** Writing – review & editing, Validation, Supervision, Data curation. **I. Jalón-Rojas:** Writing – review & editing, Validation. **T.H.M. van Emmerik:** Writing – review & editing, Validation, Supervision, Project administration, Data curation, Conceptualization.

Declaration of generative AI use

ChatGPT has been used as an inspiration to write and improve code in R.

Declaration of competing interest

The authors declare that they have no known competing financial interests or personal relationships that could have appeared to influence the work reported in this paper.

Acknowledgments

We thank the reviewers for their positive and constructive feedback, which helped improving the manuscript.

Data and code availability

The data and model used in this study is available on 4TU.ResearchData (van Waterschoot et al., 2025). Full URL: https://data.4tu.nl/datasets/08735cb7-8859-4ddb-8a09-90df4d4ba1c1.

References

Al-Thawadi, S., 2020. Microplastics and nanoplastics in aquatic environments: Challenges and threats to aquatic organisms. http://dx.doi.org/10.1007/s13369-020-04402-z.

Amaral, F.R.D., Gratiot, N., Pellarin, T., Tu, T.A., 2023. Assessing typhoon-induced compound flood drivers: a case study in Ho Chi Minh city, Vietnam. Nat. Hazards Earth Syst. Sci. 23, 3379–3405. http://dx.doi.org/10.5194/nhess-23-3379-2023.

Ashworth, P.J., Best, J.L., Parsons, D.R., 2015. Fluvial-Tidal Sedimentology, vol. 68, Elsevier, http://dx.doi.org/10.1016/c2014-0-01679-6.

Biltcliff-Ward, A., Stead, J.L., Hudson, M.D., 2022. The estuarine plastics budget: A conceptual model and meta-analysis of microplastic abundance in estuarine systems. Estuar. Coast. Shelf Sci. 275, http://dx.doi.org/10.1016/j.ecss.2022.107963.

Blondel, E., Buschman, F.A., 2022. Vertical and horizontal plastic litter distribution in a bend of a tidal river. Front. Environ. Sci. 10, http://dx.doi.org/10.3389/fenvs.2022.861457.

Boon, A., Buschman, F.A., van Emmerik, T.H.M., Broere, S., Vermeulen, B., 2023. Detection of suspended macroplastics using acoustic doppler current profiler (ADCP) echo. Front. Earth Sci. 11, http://dx.doi.org/10.3389/feart.2023.1231595.

Camenen, B., Gratiot, N., Cohard, J.a., Gard, F., Tran, V., Nguyen, A.t., Dramais, G., van Emmerik, T., Némery, J., 2020. Monitoring discharge in a tidal river using water level observations: Application to the Saigon river, Vietnam. Sci. Total. Environ. 761, 143195. http://dx.doi.org/10.1016/j.scitotenv.2020.143195.

Chae, Y., An, Y.J., 2017. Effects of micro- and nanoplastics on aquatic ecosystems: Current research trends and perspectives. Marine Poll. Bull. 124, 624–632. http://dx.doi.org/10.1016/j.marpolbul.2017.01.070.

Climo, J.D., Oswald, S.B., Buschman, F.A., Hendriks, A.J., Collas, F.P.L., 2022. Inland navigation contributes to the remobilization of land-based plastics into riverine systems. Front. Water 4, http://dx.doi.org/10.3389/frwa.2022.888091.

Cohen, J.H., Internicola, A.M., Mason, R.A., Kukulka, T., 2019. Observations and simulations of microplastic debris in a tide, wind, and freshwater-driven estuarine environment: The delaware bay. Environ. Sci. Technol. 53, 14204–14211. http://dx.doi.org/10.1021/acs.est.9b04814.

Council, W.S., 2026. Top 50 container ports. URL https://www.worldshipping.org/top-50-container-ports.

Cox, J.R., Huismans, Y., Knaake, S., Leuven, J., Vellinga, N., Van der Vegt, M., Hoitink, A., Kleinhans, M., 2021. Anthropogenic effects on the contemporary sediment budget of the lower rhine-meuse delta channel network. Earth's Futur. 9, e2020EF001869.

Crystal-Ornelas, R., Varadharajan, C., O'Ryan, D., Beilsmith, K., Bond-Lamberty, B., Boye, K., Burrus, M., Cholia, S., Christianson, D.S., Crow, M., Damerow, J., Ely, K.S., Goldman, A.E., Heinz, S.L., Hendrix, V.C., Kakalia, Z., Mathes, K., O'Brien, F., Pennington, S.C., Robles, E., Rogers, A., Simmonds, M., Velliquette, T., Weisenhorn, P., Welch, J.N., Whitenack, K., Agarwal, D.A., 2022. Enabling FAIR data in earth and environmental science with community-centric (meta)data reporting formats. Sci. Data 9, 700. http://dx.doi.org/10.1038/s41597-022-01606-w.

De Ruijsscher, T., 2016. A1: Hydraulics and morphology of longitudinal training dams. In: Hulscher, S., Schielen, R., Augustijn, D. (Eds.), RiverCare Knowledge Dissemination Days 2016: Two-Pagers of All Subprojects. STOWA, Amersfoort, The Netherlands, URL https://www.stowa.nl/sites/default/files/assets/PROJECTEN/Projecten%202020/RiverCare%20KDD%202016.pdf, subproject A1, page 11.

Defontaine, S., Sous, D., Tesan, J., Monperrus, M., Lenoble, V., Lanceleur, L., 2020. Microplastics in a salt-wedge estuary: Vertical structure and tidal dynamics. Marine Poll. Bull. 160, 111688. http://dx.doi.org/10.1016/j.marpolbul.2020.111688.

Díez-Minguito, M., Bermúdez, M., Gago, J., Carretero, O., Viñas, L., 2020. Observations and idealized modelling of microplastic transport in estuaries: The exemplary case of an upwelling system (Ría de Vigo, nw Spain). Mar. Chem. 222, http://dx.doi.org/10.1016/j.marchem.2020.103780.

Duncan, E.M., Davies, A., Brooks, A., Chowdhury, G.W., Godley, B.J., Jambeck, J., Maddalene, T., Napper, I., Nelms, S.E., Rackstraw, C., Koldewey, H., 2020. Message in a bottle: Open source technology to track the movement of plastic pollution. PLoS One 15, e0242459. http://dx.doi.org/10.1371/journal.pone.0242459.

Friedrichs, C.T., Aubrey, D.G., 1988. Non-linear tidal distortion in shallow well-mixed estuaries: a synthesis. Estuar. Coast. Shelf Sci. 27, 521–545. http://dx.doi.org/10.1016/0272-7714(88)90082-0.

Gallitelli, L., Cutini, M., Cesarini, G., Scalici, M., 2024. Riparian vegetation entraps macroplastics along the entire river course: Implications for eco-safety activities and mitigation strategies. Environ. Res. 263, 120224. http://dx.doi.org/10.1016/j.envres.2024.120224.

Geyer, W.R., MacCready, P., 2013. The estuarine circulation. Annu. Rev. Fluid Mech. 46, 175–197. http://dx.doi.org/10.1146/annurev-fluid-010313-141302, URL https://doi.org/10.1146/annurev-fluid-010313-141302.

Grosfeld, J., Schoor, M., Taormina, R., Luxemburg, W., Collas, F., 2024. Macrolitter budget and spatial distribution in a groyne field along the waal river. Marine Poll. Bull. 200, 116110. http://dx.doi.org/10.1016/j.marpolbul.2024.116110.

Hauk, R., Schreyers, L.J., Van Der Ploeg, M., Teuling, A.J., Wallerstein, N., van Emmerik, T.H.M., 2026. Preferential deposition of macroplastic on floodplains. Prepr. Res. Sq. http://dx.doi.org/10.21203/rs.3.rs-8900012/v1.

Hauk, R., Van Der Ploeg, M., Teuling, A.J., De Winter, W., van Emmerik, T.H.M., 2024. Flood-induced buttertub spill reveals riverine macroplastic transport dynamics. Environ. Sci. Eur. 36, http://dx.doi.org/10.1186/s12302-024-00962-1.

Jalón-Rojas, I., Defontaine, S., Bermúdez, M., Díez-Minguito, M., 2024. Transport of Microplastic Debris in Estuaries. Elsevier, http://dx.doi.org/10.1016/b978-0-323-90798-9.00022-6.

Jones, J.E., Hales, R.C., Larco, K., Nelson, E.J., Ames, D.P., Jones, N.L., Iza, M., 2023. Building and validating multidimensional datasets in hydrology for data and mapping web service compliance. Water 15, 411. http://dx.doi.org/10.3390/w15030411.

Kaimathuruthy, B.J., Jalón-Rojas, I., Sous, D., 2025. Modelling microplastic dynamics in estuaries: a comprehensive review, challenges, and recommendations. Geosci. Model. Dev. 18, 7227–7255. http://dx.doi.org/10.5194/gmd-18-7227-2025.

Kaimathuruthy, B.J., Jalón-Rojas, I., Sous, D., Marieu, V., Huybrechts, N., 2026. Physical drivers of transport, dispersion and trapping of microplastics in a macrotidal, hyper-turbid fluvial–estuarine system: a modelling approach. Mar. Pollut. Bull. Press.

Kuizenga, B., Tasseron, P.F., Wendt-Potthoff, K., van Emmerik, T.H.M., 2023. From source to sea: Floating macroplastic transport along the Rhine river. Front. Environ. Sci. 11, http://dx.doi.org/10.3389/fenvs.2023.1180872.

Lahens, L., Strady, E., Kieu-Le, T.C., Dris, R., Boukerma, K., Rinnert, E., Gasperi, J., Tassin, B., 2018. Macroplastic and microplastic contamination assessment of a tropical river (Saigon River, Vietnam) transversed by a developing megacity. Environ. Pollut. 236, 661–671. http://dx.doi.org/10.1016/j.envpol.2018.02.005.

Ledieu, L., Tramoy, R., Mabilais, D., Ricordel, S., Verdier, L., Tassin, B., Gasperi, J., 2022. Macroplastic transfer dynamics in the loire estuary: Similarities and specificities with macrotidal estuaries. Marine Poll. Bull. 182, 114019. http://dx.doi.org/10.1016/j.marpolbul.2022.114019.

López, A.G., Najjar, R.G., Friedrichs, M.A., Hickner, M.A., Wardrop, D.H., 2021. Estuaries as filters for riverine microplastics: Simulations in a large, coastal-plain estuary. Front. Mar. Sci. 8, http://dx.doi.org/10.3389/fmars.2021.715924.

Lotcheris, R.A., Schreyers, L.J., Bui, T.K., Thi, K.V., Nguyen, H.Q., Vermeulen, B., van Emmerik, T.H.M., 2024. Plastic does not simply flow into the sea: River transport dynamics affected by tides and floating plants. Environ. Pollut. 345, http://dx.doi.org/10.1016/j.envpol.2024.123524.

Lucie, T., Philippe, A., Laura, D.F., Arnaud, H., Matthieu, W., Julien, G., Ika, P.P., 2024. The largest estuary on the planet is not spared from plastic pollution: Case of the st. lawrence river estuary. Marine Poll. Bull. 206, http://dx.doi.org/10.1016/j.marpolbul.2024.116780.

MacCready, P., Hetland, R.D., Geyer, W., 2002. Long-term isohaline salt balance in an estuary. http://dx.doi.org/10.1016/s0278-4343(02)00023-7.

Maharjan, N., Miyazaki, H., Pati, B.M., Dailey, M.N., Shrestha, S., Nakamura, T., 2022. Detection of river plastic using uav sensor data and deep learning. Remote. Sens. 14, http://dx.doi.org/10.3390/rs14133049.

Maldegem, D.C., Mulder, H.P.J., Langerak, A., 1993. A cohesive sediment balance for the scheldt estuary. http://dx.doi.org/10.1007/bf02334788.

Naidoo, T., Glassom, D., Smit, A.J., 2015. Plastic pollution in five urban estuaries of kwazulu-natal, south africa. Marine Poll. Bull. 101, 473–480. http://dx.doi.org/10.1016/j.marpolbul.2015.09.044.

Nguyen, K.L.P., Bui, T.K.L., 2023. Riverbank macro-litters monitoring in downstream of saigon river, Ho Chi Minh city. Case Stud. Chem. Environ. Eng. 7, 100306. http://dx.doi.org/10.1016/j.cscee.2023.100306.

Nguyen, A., Némery, J., Gratiot, N., Garnier, J., Dao, T., Thieu, V., Laruelle, G., 2021. Biogeochemical functioning of an urbanized tropical estuary: Implementing the generic C-GEM (reactive transport) model. Sci. Total. Environ. 784, 147261. http://dx.doi.org/10.1016/j.scitotenv.2021.147261.

Osei-Twumasi, A., Falconer, R.A., Bockelmann-Evans, B.N., 2014. Experimental studies on water and solute transport processes in a hydraulic model of the Severn Estuary, UK. Water Resour. Manag. 29, 1731–1748. http://dx.doi.org/10.1007/s11269-014-0908-4.

Port of Rotterdam, 2025. Feiten en cijfers - de rotterdamse haven in cijfers. URL https://www.portofrotterdam.com/nl/online-beleven/feiten-en-cijfers.

Prikhodko, P., Kotlyarov, N., 2018. Calibration of sobol indices estimates in case of noisy output. URL https://arxiv.org/abs/1804.00766.

Queiroz, A.H.B., Callado, M.A.V., Rollnic, M., 2026. Macroplastic fate and transport in an amazonian estuarine system: A lagrangian modelling approach. Preprint.

Rijkswaterstaat, 0000. Monitoren Van plastic in rivieren, URL https://www.afvalcirculair.nl/zwerfafval-microplastics/riviermonitoring/.

Roebroek, C.T., Laufkötter, C., González-Fernández, D., van Emmerik, T.H.M., 2022. The quest for the missing plastics: Large uncertainties in river plastic export into the sea. Environ. Pollut. 312, 119948. http://dx.doi.org/10.1016/j.envpol.2022.119948.

Rosa, G.P., Costa, M.S., Monteiro, S.M., 2023. Do urban rivers in the amazon coast trap macroplastic? Marine Poll. Bull. 189, http://dx.doi.org/10.1016/j.marpolbul.2023.114757.

Rotterdam, Gemeente, 2024. Onderzoek010 - bevolking - rotterdam. URL https://onderzoek010.nl/dashboard/onderzoek010/bevolking.

Schernewski, G., Radtke, H., Robbe, E., Haseler, M., Hauk, R., Meyer, L., Piehl, S., Riedel, J., Labrenz, M., 2021. Emission, transport, and deposition of visible plastics in an estuary and the baltic sea—a monitoring and modeling approach. Environ. Manag. 68, 860–881. http://dx.doi.org/10.1007/s00267-021-01534-2.

Schreyers, L.J., van Emmerik, T.H.M., Bui, T.K.L., Van Thi, K.L., Vermeulen, B., Nguyen, H.Q., Wallerstein, N., Uijlenhoet, R., Van Der Ploeg, M., 2024b. River plastic transport affected by tidal dynamics. Hydrol. Earth Syst. Sci. 28, 589–610. http://dx.doi.org/10.5194/hess-28-589-2024.

Schreyers, L.J., van Emmerik, T.H.M., Huthoff, F., Collas, F.P., Wegman, C., Vriend, P., Boon, A., De Winter, W., Oswald, S.B., Schoor, M.M., Wallerstein, N., Van Der Ploeg, M., Uijlenhoet, R., 2024a. River plastic transport and storage budget. Water Res. 259, 121786. http://dx.doi.org/10.1016/j.watres.2024.121786.

Tasseron, P.F., van Emmerik, T.H.M., De Winter, W., Vriend, P., Van Der Ploeg, M., 2024. Riverbank plastic distributions and how to sample them. Microplastics Nanoplastics 4, http://dx.doi.org/10.1186/s43591-024-00100-x.

Tramoy, R., Gasperi, J., Colasse, L., Silvestre, M., Dubois, P., Noûs, C., Tassin, B., 2020. Transfer dynamics of macroplastics in estuaries – new insights from the seine estuary: Part 2. short-term dynamics based on gps-trackers. Marine Poll. Bull. 160, http://dx.doi.org/10.1016/j.marpolbul.2020.111566.

van Emmerik, T.H.M., De Lange, S., Frings, R., Schreyers, L., Aalderink, H., Leusink, J., Begemann, F., Hamers, E., Hauk, R., Janssens, N., Jansson, P., Joosse, N., Kelder, D., Van Der Kuijl, T., Lotcheris, R., Löhr, A., Mellink, Y., Pinto, R., Tasseron, P., Vos, V., Vriend, P., 2022. Hydrology as a driver of floating river plastic transport. http://dx.doi.org/10.1029/2022ef002811.

van Emmerik, T.H.M., Janssen, T.W., Jia, T., Bui, T.K.L., Taormina, R., Nguyen, H.Q., Schreyers, L.J., 2025. Plastic pollution and water hyacinths consistently co-occur in the lower Saigon riv. Environ. Res.: Wate http://dx.doi.org/10.1088/3033-4942/ae10d7.

van Emmerik, T.H.M., Kieu-Le, T.C., Loozen, M., Van Oeveren, K., Strady, E., Bui, X.T., Egger, M., Gasperi, J., Lebreton, L., Nguyen, P.D., Schwarz, A., Slat, B., Tassin, B., 2018. A methodology to characterize riverine macroplastic emission into the ocean. Front. Mar. Sci. 5, http://dx.doi.org/10.3389/fmars.2018.00372.

van Emmerik, T.H.M., Roebroek, C., De Winter, W., Vriend, P., Boonstra, M., Hougee, M., 2020a. Riverbank macrolitter in the Dutch Rhine–Meuse delta. Environ. Res. Lett. 15, 104087. http://dx.doi.org/10.1088/1748-9326/abb2c6.

van Emmerik, T.H.M., Schwarz, A., 2020. Plastic debris in rivers. Wiley Interdiscip. Rev.: Water 7, 1–24. http://dx.doi.org/10.1002/wat2.1398.

van Emmerik, T.H.M., Strady, E., Kieu-Le, T.C., Nguyen, L., Gratiot, N., 2019. Seasonality of riverine macroplastic transport. Sci. Rep. 9, 13549. http://dx.doi.org/10.1038/s41598-019-50096-1.

van Lieshout, C., van Oeveren, K., van Emmerik, T.H.M., Postma, E., 2020. Automated river plastic monitoring using deep learning and cameras. Earth Space Sci. 7, http://dx.doi.org/10.1029/2019EA000960.

van Waterschoot, D., Tas, S., Gratiot, N., Vriend, P., Rálon Rojas, R., van Emmerik, T.H.M., 2025. Dataset underlying the publication: Estimating plastic export from estuaries into the sea using a mass-balance model. http://dx.doi.org/10.4121/08735cb7-8859-4ddb-8a09-90df4d4ba1c1.v1.

Vriend, P., Schoor, M., Rus, M., Oswald, S.B., Collas, F.P., 2023. Macroplastic concentrations in the water column of the river Rhine increase with higher discharge. Sci. Total. Environ. 900, 165716. http://dx.doi.org/10.1016/j.scitotenv.2023.165716.

Vriend, P., Van Calcar, C., Kooi, M., Landman, H., Pikaar, R., van Emmerik, T.H.M., 2020. Rapid assessment of floating macroplastic transport in the Rhine. Front. Mar. Sci. 7, http://dx.doi.org/10.3389/fmars.2020.00010.

Wang, T., Zhao, S., Zhu, L., McWilliams, J.C., Galgani, L., Amin, R.M., Nakajima, R., Jiang, W., Chen, M., 2022. Accumulation, transformation and transport of microplastics in estuarine fronts. Nat. Rev. Earth Environ. 3, 795–805. http://dx.doi.org/10.1038/s43017-022-00349-x.

Wilhelm, M.F., Koopman, J., Vermeer, P., 2022. Meetmethode beeldkwaliteit zwerfafval oevers vanaf het water: Opzet van de monitoring beeldkwaliteit zwerfafval op oevers van rijkswateren vanaf een varend schip. Report R001-1285491-V02, TAUW, In opdracht van Rijkswaterstaat WVL.

Willis, K.A., Eriksen, R., Wilcox, C., Hardesty, B.D., 2017. Microplastic distribution at different sediment depths in an urban estuary. Front. Mar. Sci. 4, http://dx.doi.org/10.3389/fmars.2017.00419.

Witczak, A., Przedpełska, L., Pokorska-Niewiada, K., Cybulski, J., 2024. Microplastics as a threat to aquatic ecosystems and human health. http://dx.doi.org/10.3390/toxics12080571.

Yadav, V., Fei, X., Arora, M., et al., 2025. Gaps in quantifying environmental losses of plastics impede effective solutions. Nat. Rev. Mater. 10, 717–719. http://dx.doi.org/10.1038/s41578-025-00802-5.